RESEARCH ARTICLE

^{11}C-PE2I and ^{18}F-Dopa PET for Assessing Progression Rate in Parkinson's: A Longitudinal Study

Weihua Li, MSc,[1†] Nick P. Lao-Kaim, MSc,[1†] Andreas A. Roussakis, MD,[1] Antonio Martín-Bastida, MD, MSc,[1] Natalie Valle-Guzman, MSc,[2] Gesine Paul, MD, PhD,[3,4] Clare Loane, PhD,[5] Håkan Widner, MD, PhD,[4] Marios Politis, MD, PhD, MRCP,[6] Tom Foltynie, MD, PhD, FRCP,[7] Roger A. Barker, PhD, MBBS, MRCP,[2] and Paola Piccini, MD, PhD, FRCP[1*]

[1]*Centre for Neurodegeneration and Neuroinflammation, Division of Brain Sciences, Imperial College London, London, UK*
[2]*John Van Geest Centre for Brain Repair, University of Cambridge, Cambridge, UK*
[3]*Translational Neurology Group, Department of Clinical Sciences, Wallenberg Neuroscience Centre, Lund University, Lund, Sweden*
[4]*Division of Neurology, Department of Clinical Sciences, Lund University, Skåne University Hospital, Lund, Sweden*
[5]*Memory Research Group, Nuffield Department of Clinical Neurosciences, Medical Science Division. University of Oxford, Oxford, UK*
[6]*Neurodegeneration Imaging Group, Department of Basic and Clinical Neuroscience, Institute of Psychiatry, Psychology and Neuroscience, King's College London, London, UK*
[7]*Sobell Department of Motor Neuroscience, UCL Institute of Neurology, National Hospital for Neurology and Neurosurgery, London, UK*

ABSTRACT: Background: ^{18}F-dopa PET measuring aromatic L-amino acid decarboxylase activity is regarded as the gold standard for evaluating dopaminergic function in Parkinson's disease. Radioligands for dopamine transporters are also used in clinical trials and for confirming PD diagnosis. Currently, it is not clear which imaging marker is more reliable for assessing clinical severity and rate of progression. The objective of this study was to directly compare ^{18}F-dopa with the highly selective dopamine transporter radioligand ^{11}C-PE2I for the assessment of motor severity and rate of progression in PD.

Methods: Thirty-three mild-moderate PD patients underwent ^{18}F-dopa and ^{11}C-PE2I PET at baseline. Twenty-three were followed up for 18.8 ± 3.4 months.

Results: Standard multiple regression at baseline indicated that ^{11}C-PE2I BP_{ND} predicted UPDRS-III and bradykinesia-rigidity scores ($P < 0.05$), whereas ^{18}F-dopa K_i did not make significant unique explanatory contributions. Voxel-wise analysis showed negative correlations between ^{11}C-PE2I BP_{ND} and motor severity across the whole striatum bilaterally. ^{18}F-Dopa K_i clusters were restricted to the most affected putamen and caudate. Longitudinally, negative correlations were found between striatal Δ^{11}C-PE2I BP_{ND}, ΔUPDRS-III, and Δbradykinesia-rigidity, whereas no significant associations were found for Δ^{18}F-dopa K_i. One cluster in the most affected putamen was identified in the longitudinal voxel-wise analysis showing a negative relationship between Δ^{11}C-PE2I BP_{ND} and Δbradykinesia-rigidity.

Conclusions: Striatal ^{11}C-PE2I appears to show greater sensitivity for detecting differences in motor severity than ^{18}F-dopa. Furthermore, dopamine transporter decline is closely associated with motor progression over time, whereas no such relationship was found with aromatic L-amino acid decarboxylase. ^{11}C-PE2I may be more effective for evaluating the efficacy of neuroprotective treatments in PD. © 2017 International Parkinson and Movement Disorder Society

Key Words: Parkinson's disease; dopamine transporter; aromatic L-amino acid decarboxylase; ^{11}C-PE2I; ^{18}F-dopa

*Correspondence to: Paola Piccini, Neurology Imaging Unit, Hammersmith Hospital, Imperial College London, London, UK; paola.piccini@imperial.ac.uk.

†Weihua Li and Nick P. Lao-Kaim contributed equally to this article

Relevant conflicts of interest/financial disclosures: None

Funding agencies: The Transeuro study received funding from an FP7 EU Consortium. The Medical Research Council (MRC) cofunded the PET scans along with the FP7 EU Consortium. An NIHR award of Biomedical Research Centre to the University of Cambridge/Addenbrooke's Hospital and Imperial College London supported part of this study. Travel of Lund patients with staff has been funded by local grants in addition to Trans-Euro (Swedish Parkinson Academy, Regional Academic Learning Grants, and Multipark).

Received: 17 January 2017; **Revised:** 29 August 2017; **Accepted:** 31 August 2017

Published online 00 Month 2017 in Wiley Online Library (wileyonlinelibrary.com). DOI: 10.1002/mds.27183

Positron emission tomography (PET) with ^{18}F-dopa has long been regarded as the gold standard for measuring the integrity of dopaminergic nerve terminals and for assessing disease severity in PD patients.[1,2] ^{18}F-Dopa, a fluorinated analogue of L-dopa, follows the same presynaptic dopamine (DA) synthesis pathway, is decarboxylated by aromatic L-amino acid decarboxylase (AADC) and stored in presynaptic vesicles as ^{18}F-labeled dopamine, thus providing an in vivo measurement of AADC activity and presynaptic DA storage capacity.[3,4] Postmortem and in vivo analysis of the human PD brain has revealed that striatal ^{18}F-dopa uptake correlates positively with nigral cell count[5] and negatively with motor symptomatology.[6-12] However, upregulation of AADC activity as a compensatory response to progressive DA cell death may result in ^{18}F-dopa overestimating nerve terminal density in early PD.[9,13-15] In addition, the AADC enzyme acts as a decarboxylation catalyst within the biosynthetic pathways of several other monoamine neurotransmitters,[15,16] within which AADC upregulation is also thought to occur.[15,17,18] Given that most AADC-containing neurons are capable of taking up and converting ^{18}F-dopa,[15,17,19-21] any alterations cannot be attributed solely to dopamine terminal dysfunction.

Other nuclear imaging studies in PD patients have used radioligands that bind to the dopamine transporter (DAT). DATs are exclusively located on dopaminergic neurons,[22] and experimental work in animal models of PD have demonstrated a close relationship between striatal DA concentration, presynaptic DAT, and nigrostriatal cell loss.[23] Thus, in contrast to AADC, DAT appears to represent a more appropriate and specific marker for studying the integrity of striatal dopaminergic innervation, although it must be noted that possible compensatory DAT downregulation may cause its underestimation.[13] The negative association between striatal DAT and motor severity is well documented using a number of DAT radioligands developed for use with PET and SPECT[24,25] including those most commonly used in studies of PD, ^{123}I-β-CIT and its fluoropropyl analogue ^{123}I-FP-CIT.[10,11,26-30] However, these radioligands also have an affinity for the serotonin (SERT) and noradrenaline (NET) transporters,[31,32] the former of which is substantially present in the human striatum,[33-35] which complicates their use as measures of PD progression.

Significant striatal AADC and DAT declines have consistently been demonstrated in several longitudinal studies using the above ligands, yet, interestingly, changes over time do not appear to correlate with changes in motor symptomatology,[1,36-40] and findings from several clinical trials demonstrated incongruity between drug-related changes in motor performance and changes in striatal ^{18}F-dopa[41,42] and ^{123}I-β-CIT[43,44] values. Given that the serotonergic and noradrenergic systems also undergo disease-related neurodegeneration in PD,[15,17,18,45-47] it is possible that a lack of specificity for the DA system may result in tracer values reflecting a composition of monoaminergic degeneration including nondopaminergic factors not directly associated with motor symptoms.

The current study directly compared the validity of AADC and DAT as biological targets for the assessment of motor severity and rate of progression in early PD patients at baseline and after 19 months of follow-up. To estimate DAT, we used ^{11}C-PE2I, a highly specific DAT radioligand that has been shown to have at least 17.5-fold greater DAT/SERT and 20-fold greater DAT/NET selectivity than β-CIT[31,32,48] and negligible competition with maprotiline and citalopram.[49-51] In humans, ^{11}C-PE2I specific to nonspecific binding is highest in the striatum and is in agreement with the known DAT distribution postmortem,[52,53] and its utility for differential diagnostics has recently been demonstrated.[54] Thus, we hypothesized that striatal DAT density, as measured using ^{11}C-PE2I, would show stronger associations with motor severity compared with AADC activity derived using ^{18}F-dopa PET.

Methods

Subjects

Thirty-three patients with idiopathic PD were included from the FP7 EC Transeuro program cohort (http://www.transeuro.org.uk/; also see Supplementary Materials 1). Of these, 23 were rescanned 18.8 ± 3.4 months later, hereafter referred to as the PD_{FU} subgroup. All patients satisfied Queen Square Brain Bank criteria for PD diagnosis.[55] Motor severity was assessed by 2 experienced raters using the motor subscore of the Unified Parkinson's Disease Rating Scale (UPDRS-III)[56,57] and the Hoehn and Yahr scale[58] in the practically defined off-medicated state (see Supplementary Table 1). Patients were excluded for dementia (Mini-Mental State Examination score < 26), atypical or secondary parkinsonism, and standard MRI exclusion criteria such as the presence of metallic implants and pregnancy. Demographic information can be seen in Table 1.

MRI and PET Procedure

All scans were conducted at Imanova (Hammersmith Hospital, London). A high-resolution volumetric T1-weighted magnetization-prepared rapid acquisition gradient-echo scan was obtained on a 3T Siemens Magnetom Trio system to aid PET registration (MPRAGE: TR, 2300 milliseconds; TE, 2.98 milliseconds; flip angle, 9°; time to inversion, 900 milliseconds; GRAPPA acceleration factor PE, 2; slice thickness, 1 mm; FoV, 240 × 25 6 mm; matrix size,

TABLE 1. Demographic and clinical information for all PD patients at baseline and for the PD_{FU} subgroup at baseline and after 18.8 ± 3.4 months of follow-up

All PD (n = 33)				
	Baseline			
Sex (M:F)	27:6			
Age (years)[a]	55.1 ± 7.0			
Disease duration (years)[a]	5.9 ± 2.2			
UPDRS-III[a]	31.9 ± 10.8			
UPDRS-III bradykinesia-rigidity[a]	22.8 ± 7.9			
UPDRS-III tremor[a]	6.4 ± 5.5			
LED[a]	651.5 ± 361.4			
H&Y scale[b]	2.0 (0.0)			
PD_{FU} (n = 23)				
	Baseline	Follow-up	Statistic	*P*
Sex (M:F)	19 : 4	19 : 4		
Age (years)[a]	55.3 ± 7.2	56.8 ± 7.1	$t(22) = 26.329$	< 0.001[c]
Disease duration (years)[a]	5.6 ± 2.0	7.2 ± 2.0	$t(22) = 26.153$	< 0.001[c]
UPDRS-III[a]	32.5 ± 11.0	36.6 ± 9.2	$t(22) = 2.266$	0.034[c]
UPDRS-III bradykinesia-rigidity[a]	22.5 ± 8.5	25.2 ± 7.6	$t(22) = 2.084$	0.049[c]
UPDRS-III tremor[a]	7.7 ± 5.1	8.9 ± 4.5	$t_{22} = 1.536$	0.139
LED[a]	667.2 ± 383.3	817.9 ± 320.0	$t_{22} = 1.692$	0.105
H&Y scale[b]	2.0 (0.0)	2.0 (0.0)	$Z = 1.7$	0.083

[a]Data are presented as mean ± SD.
[b]Data are presented as median (interquartile range),
[c]$P < 0.05$.
LED, L-dopa-equivalent dose (mg); UPDRS, Unified Parkinson's disease rating scale; H&Y scale, Hoehn and Yahr scale.
The UPDRS and H&Y scale were assessed in the practically defined off-medication state.
For the PD_{FU} subgroup, Wilcoxon signed rank and paired *t*-tests were used to assess the difference between baseline and follow-up.

240 × 256 mm). One whole-brain volume was acquired consisting of 160 slices lasting 301 seconds.

^{18}F-Dopa ([^{18}F]6-fluoro-L-3,4-dihydroxyphenylalanine) and ^{11}C-PE2I ([^{11}C]N-(3-iodopro-2*E*-enyl)-2β-carbomethoxy-3β-(4′-methylphenyl)nortropane) PET scans were acquired on a Siemens Biograph TruePoint HI-REZ 6 PET/CT system on 2 consecutive days to negate cross-tracer contamination. Patients were positioned supine and movement minimized using memory foam padding. Radioligand volumes (^{11}C-PE2I, 350 MBq; ^{18}F-dopa, 180 MBq) were prepared to 10 mL using saline solution and administered intravenously as single bolus injections followed immediately by a 10-mL saline flush. Administration was at 1 mL/s. Dynamic emission data were acquired continuously for 90 minutes postinjection, then reconstructed into 26 temporal frames using a filtered back-projection algorithm (direct inversion Fourier transform; matrix size, 128 × 128; zoom, 2.6; 5 mm transaxial Gaussian filter; pixel size, 2 mm isotropic). A low-dose CT transmission scan (0.36 mSv) was acquired for attenuation correction. Patients withdrew dopaminergic medication 24 hours prior to scanning for standard release and 48 hours for prolonged release preparations. For ^{18}F-dopa, a 150-mg oral dose of carbidopa was administered 1 hour prior to injection.

Data were collected under the Transeuro study, funded by FP7 and carried out in accordance with the Declaration of Helsinki, after approval from the appropriate research ethics committees of the UK (REC 12/EE/0096 and 10/H0805/73) and Sweden (EPN 2013/758 and IK 2013/685) National Research Ethics Service Committee. All patients gave written informed consent before participation.

Image Preprocessing

PET and MRI images were preprocessed and analyzed using MIAKAT v3.4.2. (Molecular Imaging and Kinetic Analysis Toolbox, Imanova Ltd., London, UK),[59] which uses FSL (FMRIB Image Analysis Group, Oxford, UK),[60] SPM (Statistical Parametric Mapping, Wellcome Trust Centre for Neuroimaging, London, UK), and in-house preprocessing and kinetic modeling procedures and implemented in MATLAB (Mathworks, Natick, MA).

Structural MPRAGE images were brain-extracted, segmented, and rigid-body-registered to the Montreal Neurological Institute (MNI) template.[61] MPRAGE images were then used to manually trace striatal regions of interest (bilateral/left/right caudate, anterior and posterior putamen) on the axial plane followed by trace checks on the coronal plane, using Analyze 11.0 (Biomedical Imaging Resource, Mayo Clinic). The putamen was subdivided based on the anterior commissure landmark.[62] The cerebellum was defined by nonlinearly registering the MNI template to MPRAGE

and applying the deformation fields to an MNI-based regional atlas (CIC Atlas v1.2; GlaxoSmithKline Clinical Imaging Centre, London, UK).[62] Rigid-body registration parameters were applied to the gray- and white-matter segmentation images to enable automatic masking of cerebellar gray matter.

Dynamic PET images were corrected for intrascan head movement using frame-to-frame rigid registration (reference frame, 16) and summed (10-90 minutes) to obtain signal-averaged (ADD) images. ADD images were coregistered to the corresponding structural MPRAGE using normalized mutual information and resultant matrices applied to the realigned dynamic PET frames so that all images were in register. Region-of-interest (ROI) maps were then overlaid onto the dynamic PET frames to obtain regional time-activity curves. For ^{11}C-PE2I, the simplified reference tissue model was used to calculate regional nondisplaceable binding potential (BP_{ND}).[63] Cerebellar gray matter was used as a reference as it has been shown to have negligible DAT density compared with other brain regions.[49,50,52] For ^{18}F-dopa, the regional influx constant (K_i) was calculated using the Patlak graphical method[64] between 30 and 90 minutes ($t^* = 30$). AADC activity in both the cerebellum and occipital cortex is assumed to be zero,[65] thus a cerebellar reference was used to maintain analytical consistency across radioligands.

Parametric images were also generated by fitting kinetic models at each voxel of the MPRAGE-registered dynamic PET series. To enable voxel-wise statistical analysis at the group level, registered gray- and white-matter segments were used to create a study-specific template using diffeomorphic anatomical registration through exponentiated Lie algebra (DARTEL), which was then normalized (affine transform) to MNI space in SPM12. Individual flow fields and normalization parameters were then applied to the corresponding parametric images while preserving concentrations to ensure PET voxel values were not modulated for volumetric changes.

ROI Analysis

All statistical analyses were performed using SPSS v22.0 (SPSS Statistics for Macintosh; IBM Corp., Armonk, NY).

Pearson's correlation coefficient was used to evaluate the relationship between bilateral striatal ^{18}F-dopa K_i and ^{11}C-PE2I BP_{ND} measures and UPDRS-III, tremor, and bradykinesia-rigidity subscores (see Supplementary Table 1) for all PD patients at baseline. Correlations between lateralized UPDRS-III, tremor, and bradykinesia-rigidity subscores (clinically most/least affected [MA/LA] sides) and contralateral PET measures were assessed using Spearman's rho, as several lateralized variables demonstrated significant deviation from normality (Shapiro-Wilk $P < 0.05$). Differences between lateralized correlation coefficients were tested using Steiger's Z procedure.[66]

Standard multiple regression was used to compare the ability of bilateral striatal ^{18}F-dopa K_i and ^{11}C-PE2I BP_{ND} to predict clinical disease severity for all PD patients at baseline. Six separate models were constructed, with each model including 2 predictor variables (^{18}F-dopa K_i and ^{11}C-PE2I BP_{ND} in either bilateral caudate, anterior or posterior putamen) and 1 dependent variable (UPDRS-III or bradykinesia-rigidity subscore). This enabled us to evaluate the independent contributions of each tracer to predict clinical severity, while the effects of the alternate predictor were held constant.

For the PD_{FU} subgroup, changes in ^{18}F-dopa K_i and ^{11}C-PE2I BP_{ND} at follow-up were assessed using the Wilcoxon signed rank test because of nonnormal data (Shapiro-Wilk $P < 0.05$). To evaluate the association of each radioligand with disease progression, difference scores were calculated (Δ: follow-up – baseline) and the relationship between changes in bilateral tracer values (Δ^{18}F-dopa K_i; Δ^{11}C-PE2I BP_{ND}) in the caudate, anterior and posterior putamen, and changes in clinical severity measures (ΔUPDRS-III; Δbradykinesia-rigidity) was assessed using Spearman's rho. Steiger's Z was used to test the difference between Δ^{18}F-dopa K_i and the corresponding Δ^{11}C-PE2I BP_{ND} correlation coefficients.

Voxel-Wise Analysis

Because PD is a highly asymmetric movement disorder, MRI and PET images for patients with more severe clinical features on the right side were left-right-flipped prior to image preprocessing. Normalized parametric images for all PD patients at baseline (n = 33) were then entered into a multiple regression model in SPM12 with UPDRS-III, tremor, and bradykinesia-rigidity subscores as covariates of interest and age and sex as nuisance covariates. For follow-up analysis (n = 23), difference maps created by voxel-wise subtraction (Δ: follow-up – baseline) were entered into a multiple regression model with ΔUPDRS-III, Δtremor, and Δbradykinesia-rigidity subscores as covariates of interest and age at baseline and sex as nuisance covariates. An explicit mask was applied to limit the analysis to the basal ganglia. Statistical inference was based on threshold-free cluster enhancement (TFCE toolbox v89 for SPM8/SPM12, http://dbm.neuro.uni-jena.de/tfce/), which uses a nonparametric permutation testing approach (5000 permutations) to produce images in which voxel-wise values are reflective of the local spatial extent and negates the need to define arbitrary initial cluster-forming thresholds.[67] Voxel-wise statistical maps were corrected for family-wise error at $P_{FWE} < 0.1$.

Results

ROI Analysis

Baseline

At baseline, ^{18}F-dopa K_i showed significant negative correlations with UPDRS-III and bradykinesia-rigidity in the posterior putamen (Fig. 1a,c). In contrast, ^{11}C-PE2I BP_{ND} showed significant negative relationships with both UPDRS-III and bradykinesia-rigidity in all striatal ROIs (Fig. 1b,d). No significant correlations were found between ^{18}F-dopa K_i and ^{11}C-PE2I BP_{ND} and tremor subscores.

Multiple regression analyses showed that all models significantly predicted UPDRS-III and bradykinesia-rigidity scores. However, only ^{11}C-PE2I BP_{ND} made significant unique contributions to the predictions in all models, apart from between anterior putamen ^{18}F-dopa K_i and ^{11}C-PE2I BP_{ND} and UPDRS-III score (Table 2). All data assumptions for standard multiple regression including those of multicollinearity were met.

Laterality analysis indicated significant negative correlations between UPDRS-III-MA ($r_s = -0.42$, $P = 0.014$) as well as bradykinesia-rigidity-MA ($r_s = -0.44$, $P = 0.011$) and contralateral posterior putamen ^{18}F-dopa K_i. No correlations were found between motor severity measures on the clinically least affected side and contralateral striatal ^{18}F-dopa K_i. For ^{11}C-PE2I BP_{ND}, significant relationships with UPDRS-III-MA (contralateral caudate: $r_s = -0.39$, $P = 0.024$; anterior putamen: $r_s = -0.37$, $P = 0.037$; posterior putamen: $r_s = -0.45$, $P = 0.008$), UPDRS-III-LA (contralateral caudate: $r_s = -0.42$, $P = 0.014$; anterior putamen: $r_s = -0.45$, $P = 0.0093$; posterior putamen: $r_s = -0.53$, $P = 0.0014$), bradykinesia-rigidity-MA (contralateral caudate: $r_s = -0.48$, $P = 0.0061$; anterior putamen: $r_s = -0.55$, $P < 0.001$; posterior putamen: $r_s = -0.62$, $P < 0.001$) and bradykinesia-rigidity-LA (contralateral caudate: $r_s = -0.48$, $P = 0.0046$; anterior putamen: $r_s = -0.53$, $P = 0.0013$; posterior putamen: $r_s = -0.63$, $P < 0.001$) were identified in all respective contralateral ROIs, although the correlation between UPDRS-III-MA and contralateral caudate ^{11}C-PE2I BP_{ND} did not survive Benjamini-Hochberg false discovery rate (FDR) correction. No significant correlations were found for tremor. Steiger's Z indicated that correlations were significantly stronger between both UPDRS-III-LA and bradykinesia-rigidity-LA and ^{11}C-PE2I BP_{ND} than the corresponding ^{18}F-dopa K_i correlations in the contralateral anterior (UPDRS-III-LA: $Z = 2.27$, $P = 0.012$; bradykinesia-rigidity-LA: $Z = 2.64$, $P = 0.0042$) and posterior putamen (UPDRS-III-LA: $Z = 1.97$, $P = 0.024$; bradykinesia-rigidity-LA: $Z = 2.06$, $P = 0.019$); see Supplementary Figure 1.

Follow-Up

For the PD_{FU} subgroup, the Wilcoxon signed rank test showed a significant decrease in anterior putaminal ^{18}F-dopa K_i ($Mdn_{Baseline}$, 0.00563; Mdn_{FU}, 0.00509; $Z = -3.194$, $r = -0.471$, $P = 0.001$) but not in the posterior putamen ($Mdn_{Baseline}$, 0.00311; Mdn_{FU}, 0.00301; $Z = -1.794$, $r = -0.265$, $P = 0.075$) or caudate ($Mdn_{Baseline}$, 0.00624; Mdn_{FU}, 0.00588; $Z = -1.855$, $r = -0.274$, $P = 0.065$). Significant decreases in ^{11}C-PE2I BP_{ND} were found in the caudate ($Mdn_{Baseline}$, 2.274; Mdn_{FU}, 2.121; $Z = -3.406$, $r = -0.502$, $P < 0.001$), posterior putamen ($Mdn_{Baseline}$, 0.896; Mdn_{FU}, 0.738; $Z = -3.711$, $r = -0.547$, $P < 0.001$), and anterior putamen ($Mdn_{Baseline}$, 1.986; Mdn_{FU}, 1.601; $Z = -3.680$, $r = -0.543$, $P < 0.001$).

Significant negative correlations were found between change in motor severity (ΔUPDRS-III; Δbradykinesia-rigidity) and Δ^{11}C-PE2I BP_{ND} in the caudate and posterior putamen (Fig. 1f,h). In the anterior putamen, Δ^{11}C-PE2I BP_{ND} significantly correlated with Δbradykinesia-rigidity; however, the correlation with ΔUPDRS-III did not survive Benjamini-Hochberg FDR. No significant correlations were evident between Δ^{18}F-dopa K_i and change in motor severity measures in any striatal ROI (Fig. 1e,g). Correlations between Δ^{11}C-PE2I BP_{ND} and ΔUPDRS-III in the caudate ($Z = 1.885$, $P < 0.05$) and anterior putamen ($Z = 1.984$, $P < 0.05$) and between Δ^{11}C-PE2I BP_{ND} and Δbradykinesia-rigidity in the caudate ($Z = 2.028$, $P < 0.05$) and anterior putamen ($Z = 2.49$, $P < 0.01$) were significantly stronger the than corresponding Δ^{18}F-dopa K_i correlations (Fig. 1e-h).

Voxel-Wise Analysis

For ^{18}F-dopa K_i, 2 small clusters showed a negative correlation with UPDRS-III score in the posterior and anterior putamen on the most affected side ($P_{FWE} < 0.1$). The association with bradykinesia-rigidity subscore revealed slightly larger clusters in the most affected posterior putamen ($P_{FWE} < 0.05$) and caudate body ($P_{FWE} < 0.1$). For ^{11}C-PE2I BP_{ND}, clusters showing significant negative correlations with UPDRS-III score were found in the most affected putamen and caudate ($P_{FWE} < 0.05$) and posterior putamen on the least affected side ($P_{FWE} < 0.1$). Negative correlations with bradykinesia-rigidity subscores revealed 2 large clusters on both the most affected side($P_{FWE} = 0.002$) and the least affected side ($P_{FWE} = 0.005$), which encompassed the putamen and caudate and extended into the ventral portion of the striatum (Fig. 2a-d, Table 3). Voxel-wise analysis of the difference maps (Δ: follow-up – baseline) revealed a single cluster in the most affected putamen showing a significant negative correlation between Δ^{11}C-PE2I BP_{ND} and Δbradykinesia-rigidity ($P_{FWE} = 0.042$); see Figure 2e and Table 3. No other significant results were found for longitudinal analysis. There were no regions showing positive correlations between ^{18}F-dopa K_i, ^{11}C-PE2I BP_{ND}, and motor severity measures. No significant clusters were found for tremor.

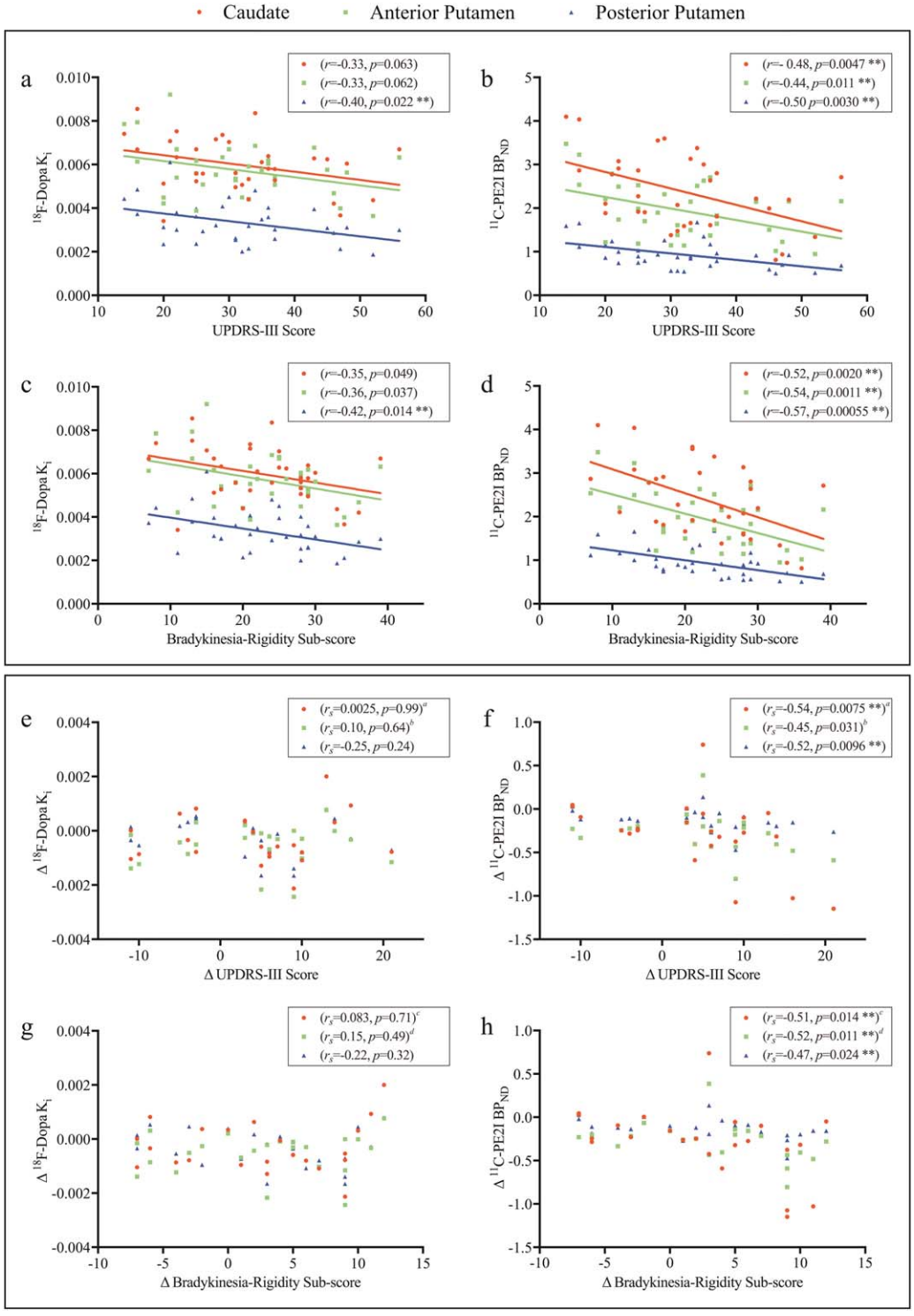

FIG. 1. (a-d) Pearson's correlations between bilateral tracer values (^{18}F-dopa K_i, ^{11}C-PE2I BP_{ND}) in the caudate, anterior and posterior putamen, and motor severity (UPDRS-III, bradykinesia-rigidity subscore) at baseline (n = 33). (e-h) Spearman's correlations between change in bilateral tracer values (Δ^{18}F-dopa K_i, Δ^{11}C-PE2I BP_{ND}) in the caudate, anterior and posterior putamen, and change in motor severity (ΔUPDRS-III, Δbradykinesia-rigidity subscore) between baseline and follow-up for the PD_{FU} subgroup are also shown (n = 23). **Significant correlation after Benjamini-Hochberg FDR correction. [a, b, c, d]Correlation pairs for which Steiger's *Z* indicated a significant difference ([a,b,c]$P < 0.05$, [d]$P < 0.01$). [Color figure can be viewed at wileyonlinelibrary.com]

Discussion

Our findings are in agreement with previous studies showing an inverse relationship between striatal ^{18}F-dopa K_i and motor severity.[2,6,8-11] However, we found that negative correlations between motor severity and striatal ^{11}C-PE2I BP_{ND} were overall stronger than the analogous ^{18}F-dopa K_i correlations. This was

TABLE 2. Standard multiple regression analysis between predictor variables ^{18}F-dopa K_i and ^{11}C-PE2I BP_{ND} in the caudate and posterior and anterior putamen and criterion variables UPDRS-III/bradykinesia-rigidity subscore for all PD patients at baseline (n = 33).

			Model fit				Estimated coefficients				
Model	Criterion	Predictors	$F_{2,30}$	P	R^2	$R^2_{adjusted}$	B	SE_B	β	t_{30}	P
1	UPDRS-III	Caudate	4.636	0.018[a]	0.236	0.185					
		^{18}F-Dopa K_i					1042.234	2214.511	0.120	0.471	0.641
		^{11}C-PE2I BP_{ND}					−7.307	3.249	−0.574	−2.249	0.032[a]
2	UPDRS-III	Anterior putamen	3.545	0.041[a]	0.191	0.137					
		^{18}F-Dopa K_i					63.194	2218.330	0.007	0.028	0.977
		^{11}C-PE2I BP_{ND}					−7.316	4.161	−0.443	−1.758	0.089
3	UPDRS-III	Posterior putamen	5.349	0.01[a]	0.263	0.214					
		^{18}F-Dopa K_i					−1618.480	2284.284	−0.142	−0.709	0.484
		^{11}C-PE2I BP_{ND}					−13.937	6.767	−0.412	−2.060	0.048[a]
4	Bradykinesia-rigidity	Caudate	5.736	0.008[a]	0.277	0.228					
		^{18}F-Dopa K_i					957.383	1591.664	0.149	0.601	0.552
		^{11}C-PE2I BP_{ND}					−5.964	2.335	−0.634	−2.554	0.016[a]
5	Bradykinesia-rigidity	Anterior putamen	6.373	0.005[a]	0.298	0.251					
		^{18}F-Dopa K_i					712.968	1526.242	0.110	0.467	0.644
		^{11}C-PE2I BP_{ND}					−7.622	2.863	−0.624	−2.663	0.012[a]
6	Bradykinesia-rigidity	Posterior putamen	7.451	0.002[a]	0.332	0.287					
		^{18}F-Dopa K_i					−950.150	1606.237	−0.113	−0.592	0.559
		^{11}C-PE2I BP_{ND}					−12.463	4.758	−0.499	−2.619	0.014[a]

R^2, coefficient of determination; $R^2_{adjusted}$, coefficient of determination adjusted for number of predictors; B, unstandardized regression coefficient; SE_B, standard error of the coefficient; β, standardized coefficient.
[a]$P < 0.05$.

further evidenced when tracers were compared directly in a multiple regression analysis, whereby ^{11}C-PE2I BP_{ND} proved to be more predictive of motor severity between patients than ^{18}F-dopa K_i. In addition, although voxel-wise analysis revealed significant clusters in both cases, at baseline the spatial extent was greater for ^{11}C-PE2I BP_{ND} than for ^{18}F-dopa K_i, encompassing the majority of the putamen bilaterally and the most affected caudate. At follow-up, only the most affected putamen showed a relationship between changes in ^{11}C-PE2I BP_{ND} in bradykinesia-rigidity. Taken together, the data suggest that DAT quantification using ^{11}C-PE2I BP_{ND} is more sensitive for investigating disease progression than ^{18}F-dopa K_i.

Although negative correlations have consistently been found between striatal presynaptic DAT density and motor severity using a number of tropane analogues[10,11,13,26-30,68,69] few have directly compared the validity of AADC and DAT imaging as biomarkers relating to the progression of disease in human PD patients. Both Eshuis et al (2006)[10] and Ishikawa et al (1996)[11] found equivalently strong relationships for

TABLE 3. Clusters showing a negative relationship between motor severity (UPDRS-III; bradykinesia-rigidity) and tracer values (^{18}F-dopa K_i; ^{11}C-PE2I BP_{ND}), as revealed by voxel-wise multiple regression analysis for all PD patients at baseline (n = 33). Longitudinal multiple regression using difference maps (Δ: follow-up – baseline) from the PD_{FU} group (*n=23*) are also shown.

Analysis	Radioligand	Motor score	k	x	y	z	P_{FWE}	Region
Baseline (n = 33)	^{18}F-Dopa K_i	UPDRS-III	80	27	−2	2	0.071	MA posterior putamen
			21	27	12	−3	0.091	MA anterior putamen
		Bradykinesia-rigidity	387	24	3	2	0.022[a]	MA posterior putamen
			79	9	8	9	0.055	MA caudate body
	^{11}C-PE2I BP_{ND}	UPDRS-III	498	9	8	8	0.027[a]	MA caudate
			889	24	0	2	0.050[a]	MA putamen
			101	−32	−18	−2	0.085	LA posterior putamen
		Bradykinesia-rigidity	2939	12	3	14	0.002[a]	MA caudate/putamen
			2083	−33	−12	−6	0.005[a]	LA caudate/putamen
Follow-up (n = 23)	Δ^{11}C-PE2I BP_{ND}	ΔBradykinesia-rigidity	397	26	14	9	0.042[a]	MA putamen

Coordinates reported in MNI space.
[a]Results significant at $P_{FWE} < 0.05$.
k, cluster size; MA, most affected side; LA, least affected side.
No clusters were identified that showed a positive correlation between motor severity and tracer values.

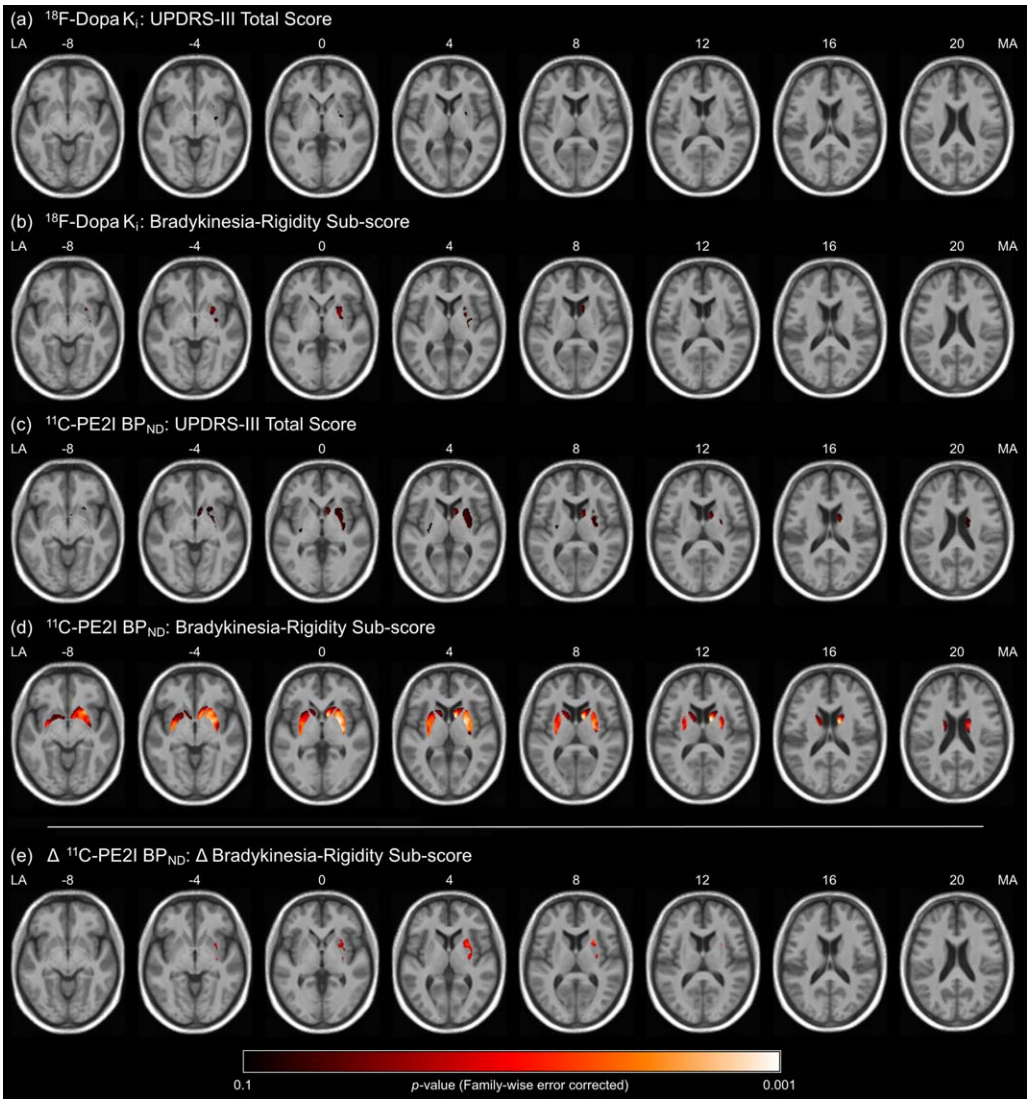

FIG. 2. Results of the voxel-wise multiple regression analysis at baseline (n = 33) showing striatal regions in which motor severity (UPDRS-III, bradykinesia-rigidity subscore) was negatively related to striatal tracer values (^{18}F-dopa K_i, ^{11}C-PE2I BP_{ND}) after correcting for age and sex (threshold-free cluster enhancement corrected at $P_{FWE} < 0.1$) (a-d). Longitudinal voxel-wise multiple regression analysis whereby the relationship between change in motor severity (ΔUPDRS-III, Δbradykinesia-rigidity subscore) and change in striatal tracer values (Δ^{18}F-dopa K_i, Δ^{11}C-PE2I BP_{ND}) was assessed using difference maps (Δ, follow-up – baseline) of the PD_{FU} subgroup (n = 23) also showed negative clusters after correcting for age at baseline and sex (threshold-free cluster enhancement corrected at $P_{FWE} < 0.1$) (e). No clusters showing positive correlations were identified. An explicit mask was applied to limit statistical analysis to the striatum. Cluster maps were overlaid onto a study-specific average template created using DARTEL in MNI coordinate space. MA, most affected side; LA, least affected side. [Color figure can be viewed at wileyonlinelibrary.com]

^{123}I-FP-CIT and ^{18}F-dopa with motor severity, whereas, interestingly, another study noted that the correlation with the DAT radioligand ^{76}Br-FE-CBT was weaker than with ^{18}F-dopa.[9]

It is possible that the differing results could be explained by the variation in affinities of DAT tracers for SERT, which, although predominantly concentrated in the raphe and thalamus, are also located in the striatum.[33-35] We are unable to comment on ^{76}Br-FE-CBT because, to our knowledge, there are no available studies describing its binding characteristics. However, autoradiographic and in vivo data indicate significant binding decreases in known SERT regions after administration of selective serotonin reuptake inhibitors (SSRI) for β-CIT, FP-CIT, and FE-CIT,[70,71] with β-CIT analogue comparison studies demonstrating DAT-to-SERT selectivity ratios of 1.68, 2.78, and 3.6, respectively.[31,32] Because serotonergic degeneration in PD is thought to follow a variable nonlinear progression[72] and is not associated with disease severity,[46] ligands with relatively low DAT-to-SERT selectivity may result in an underestimation of the association between DAT and motor severity when the influence of SERT is not accounted for. In contrast, some studies reported that PE2I may have up to 29.4 times greater selectivity for DAT over SERT.[48,73]

PE2I appears to be unaltered by SSRI competition,[49,50] and 1 study directly comparing striatal ^{123}I-PE2I and ^{123}I-FP-CIT binding found no significant change by citalopram infusion for the former but a 24% decrease for the latter.[51] Our findings may reflect this selectivity difference, although it should be noted that we did not directly compare ^{11}C-PE2I with other DAT ligands in the current study.

We observed that longitudinal changes in motor severity were not associated with changes in ^{18}F-dopa uptake, replicating previous findings.[36,39,40] In contrast, changes in motor severity were related to changes in ^{11}C-PE2I binding, suggesting that motor progression is more closely correlated to striatal DAT decline than to AADC activity. Other longitudinal studies using ^{123}I-β-CIT SPECT to quantify alterations in DAT density over time have previously failed to demonstrate this relationship with motor progression.[37,38] The current results could therefore be explained by differing serotonergic and noradrenergic contributions to tracer signal. There is also evidence to suggest that AADC activity is upregulated in early PD as a compensatory mechanism for the loss of DA nerve terminals.[9,13-15] In theory, this would result in ^{18}F-dopa underestimating the rate of dopaminergic neurodegeneration, which in turn could potentially confound associations with symptom severity. However, it is worth noting that DAT downregulation is also hypothesized to occur to maintain substantial DA levels in the synapse,[13] which could similarly affect the symptomatic relationships with ^{11}C-PE2I, albeit through overestimating the rate of denervation.

Nonetheless, other ^{18}F-dopa PET studies examining extrastriatal alterations in early PD have identified additional increases in regions known to possess high concentrations of serotonergic and noradrenergic neurons, such as the raphe complex and locus coeruleus,[15,17,18] indicating that AADC upregulation is not restricted solely to dopaminergic neurons. The ubiquitous availability of AADC and its upregulation across monoaminergic neurons constitute a bias away from accurate estimation of DA-specific progression, which to some degree may perturb the relationship between ^{18}F-dopa and motor severity. In our longitudinal cohort, we observed a trend toward a lesser annual decline rate for ^{18}F-dopa as compared with ^{11}C-PE2I (see Supplementary Table 2), which would lend partial support to this theory. However, we caution that evidence for this mismatch was not statistically strong, and it is possible that a delay of approximately 18 months was not enough to afford adequate power for robust detection. A greater understanding could be gained by further repeated measurements and/or extending the length of time between examinations.

Our results have important implications for the use of molecular imaging to monitor the progression of underlying PD pathology. Of particular interest is their potential for providing objective indices on the rate of nigrostriatal degeneration in clinical trials involving novel drug treatments and neuroprotective and neuromodulatory therapies. Several double-blind, randomized, controlled trials utilizing ^{18}F-dopa PET and ^{123}I-β-CIT SPECT to compare the long-term neurological effects of L-dopa and dopamine agonists have previously reported discordance between clinical and neuroimaging findings. Whereas PD patients taking L-dopa exhibited a slowing of clinical progression compared with those taking ropinirole[41,42] or pramipexole,[44,74] the L-dopa groups showed greater reductions in striatal DAT (^{123}I-β-CIT) and AADC activity (^{18}F-dopa). These data could reflect a paradoxical medication-related effect, yet the possible serotonergic contribution to ^{18}F-dopa and ^{123}I-β-CIT signals[31,32,48,70,73] makes it difficult to attribute drug-induced striatal changes to modifications of the dopaminergic system alone.

^{11}C-PE2I has limitations; the short half-life of ^{11}C essentially restricts its use to centers with in-house production facilities,[54] and the requirement that scanning time be >70 minutes to reliably estimate striatal DAT[75] may increase head movement and patient discomfort. In addition, its test-retest variability has been shown to be approximately double that of ^{18}F-dopa (4.52% vs 9.8% in the striatum),[75,76] which makes changes in the short-term more difficult to detect and restricts its case-by-case application. However, the ability of ^{11}C-PE2I to track changes in motor performance over time, as demonstrated here, and its favorable DAT selectivity[48-51,73] illustrates its potential as an alternative surrogate biomarker for studies of PD progression.

In conclusion, we have shown that striatal DAT density, as measured using ^{11}C-PE2I, has greater predictive value and sensitivity for detecting differences in motor severity in early-moderate PD patients than AADC imaging using ^{18}F-dopa. Furthermore, our results indicate that DAT decline is closely associated with motor progression over time, whereas no such relationship was found with AADC. These findings provide further evidence of the utility of ^{11}C-PE2I as an objective biomarker for investigating the effects of novel interventions on the rate of nigrostriatal degeneration in PD. ■

Acknowledgments: This article presents independent research funded by the FP7 EU Consortium and the MRC that is supported by the NIHR CRF and BRC at Imperial College Healthcare NHS Trust. The views expressed are those of the authors and not necessarily those of the funder, the NHS, the NIHR, or the Department of Health. This work was also supported financially by a PhD studentship awarded to N.P.L.K. from Parkinson's UK. We are very grateful to the patients who took part in this study.

References

1. Morrish PK, Sawle GV, Brooks DJ. An [18F]dopa-PET and clinical study of the rate of progression in Parkinson's disease. Brain 1996; 119(Pt 2):585-591.
2. Punal-Rioboo J, Serena-Puig A, Varela-Lema L, Alvarez-Paez AM, Ruano-Ravina A. Clinical utility of (18)F-DOPA-PET in movement disorders. A systematic review. Rev Esp Med Nucl 2009;28:106-113.
3. Kuwabara H, Cumming P, Reith J, et al. Human striatal L-dopa decarboxylase activity estimated in vivo using 6-[18F]fluoro-dopa and positron emission tomography: error analysis and application to normal subjects. J Cereb Blood Flow Metab 1993;13:43-56.
4. Heiss WD, Hilker R. The sensitivity of 18-fluorodopa positron emission tomography and magnetic resonance imaging in Parkinson's disease. Eur J Neurol 2004;11:5-12.
5. Snow BJ, Tooyama I, McGeer EG, et al. Human positron emission tomographic [18F]fluorodopa studies correlate with dopamine cell counts and levels. Ann Neurol 1993;34:324-330.
6. Brooks DJ, Ibanez V, Sawle GV, et al. Differing patterns of striatal 18F-dopa uptake in Parkinson's disease, multiple system atrophy, and progressive supranuclear palsy. Ann Neurol 1990;28:547-555.
7. Vingerhoets FJ, Schulzer M, Calne DB, Snow BJ. Which clinical sign of Parkinson's disease best reflects the nigrostriatal lesion? Ann Neurol 1997;41:58-64.
8. Broussolle E, Dentresangle C, Landais P, et al. The relation of putamen and caudate nucleus 18F-Dopa uptake to motor and cognitive performances in Parkinson's disease. J Neurol Sci 1999;166: 141-151.
9. Ribeiro MJ, Vidailhet M, Loc'h C, et al. Dopaminergic function and dopamine transporter binding assessed with positron emission tomography in Parkinson disease. Arch Neurol 2002;59:580-586.
10. Eshuis SA, Maguire RP, Leenders KL, Jonkman S, Jager PL. Comparison of FP-CIT SPECT with F-DOPA PET in patients with de novo and advanced Parkinson's disease. Eur J Nucl Med Mol Imaging 2006;33:200-209.
11. Ishikawa T, Dhawan V, Kazumata K, et al. Comparative nigrostriatal dopaminergic imaging with iodine-123-beta CIT-FP/SPECT and fluorine-18-FDOPA/PET. J Nucl Med 1996;37:1760-1765.
12. Nandhagopal R, Kuramoto L, Schulzer M, et al. Longitudinal progression of sporadic Parkinson's disease: a multi-tracer positron emission tomography study. Brain 2009;132:2970-2979.
13. Lee CS, Samii A, Sossi V, et al. In vivo positron emission tomographic evidence for compensatory changes in presynaptic dopaminergic nerve terminals in Parkinson's disease. Ann Neurol 2000; 47:493-503.
14. Tedroff J, Ekesbo A, Rydin E, Langstrom B, Hagberg G. Regulation of dopaminergic activity in early Parkinson's disease. Ann Neurol 1999;46:359-365.
15. Pavese N, Rivero-Bosch M, Lewis SJ, Whone AL, Brooks DJ. Progression of monoaminergic dysfunction in Parkinson's disease: a longitudinal 18F-dopa PET study. Neuroimage 2011;56:1463-1468.
16. Fischman AJ. Role of [18F]-dopa-PET imaging in assessing movement disorders. Radiol Clin North Am 2005;43:93-106.
17. Rakshi JS, Uema T, Ito K, et al. Frontal, midbrain and striatal dopaminergic function in early and advanced Parkinson's disease A 3D [(18)F]dopa-PET study. Brain 1999;122(Pt 9):1637-1650.
18. Moore RY, Whone AL, Brooks DJ. Extrastriatal monoamine neuron function in Parkinson's disease: An 18F-dopa PET study. Neurobiol Dis 2008;29:381-390.
19. Brown WD, Taylor MD, Roberts AD, et al. FluoroDOPA PET shows the nondopaminergic as well as dopaminergic destinations of levodopa. Neurology 1999;53:1212-1218.
20. Moore RY, Whone AL, McGowan S, Brooks DJ. Monoamine neuron innervation of the normal human brain: an 18F-DOPA PET study. Brain Res 2003;982:137-145.
21. Pavese N, Simpson BS, Metta V, Ramlackhansingh A, Chaudhuri KR, Brooks DJ. [18F]FDOPA uptake in the raphe nuclei complex reflects serotonin transporter availability. A combined [18F]FDOPA and [11C]DASB PET study in Parkinson's disease. Neuroimage 2012;59:1080-1084.
22. Becker G, Muller A, Braune S, et al. Early diagnosis of Parkinson's disease. J Neurol 2002;249(Suppl 3):III/40-48.
23. Bezard E, Dovero S, Prunier C, et al. Relationship between the appearance of symptoms and the level of nigrostriatal degeneration in a progressive 1-methyl-4-phenyl-1,2,3,6-tetrahydropyridine-lesioned macaque model of Parkinson's disease. J Neurosci 2001; 21:6853-6861.
24. Shih MC, Amaro E, Ferraz HB, et al. Neuroimaging of the dopamine transporter in Parkinson's disease: first study using [Tc-99m]-TRODAT-1 and SPECT in Brazil. Arq Neuropsiquiatr 2006;64: 628-634.
25. Wu XA, Cai HW, Ge R, Li L, Jia ZY. Recent Progress of Imaging Agents for Parkinson's Disease. Current Neuropharmacology 2014;12:551-563.
26. Seibyl JP, Marek KL, Quinlan D, et al. Decreased single-photon emission computed tomographic [123I]beta-CIT striatal uptake correlates with symptom severity in Parkinson's disease. Ann Neurol 1995;38:589-598.
27. Pirker W. Correlation of dopamine transporter imaging with parkinsonian motor handicap: how close is it? Mov Disord 2003; 18(Suppl 7):S43-S51.
28. Benamer HT, Patterson J, Wyper DJ, Hadley DM, Macphee GJ, Grosset DG. Correlation of Parkinson's disease severity and duration with 123I-FP-CIT SPECT striatal uptake. Mov Disord 2000; 15:692-698.
29. Wang J, Zuo CT, Jiang YP, et al. 18F-FP-CIT PET imaging and SPM analysis of dopamine transporters in Parkinson's disease in various Hoehn & Yahr stages. J Neurol 2007;254:185-190.
30. Ottaviani S, Tinazzi M, Pasquin I, et al. Comparative analysis of visual and semi-quantitative assessment of striatal [123I]FP-CIT-SPET binding in Parkinson's disease. Neurol Sci 2006;27:397-401.
31. Abi-Dargham A, Gandelman MS, DeErausquin GA, et al. SPECT imaging of dopamine transporters in human brain with iodine-123-fluoroalkyl analogs of beta-CIT. J Nucl Med 1996;37:1129-1133.
32. Neumeyer JL, Wang SY, Gao YG, et al. N-omega-fluoroalkyl analogs of (1r)-2-beta-carbomethoxy-3-beta-(4-iodophenyl)-tropane (beta-cit) — radiotracers for positron emission tomography and single-photon emission computed-tomography imaging of dopamine transporters. J Med Chem 1994;37:1558-1561.
33. Ichise M, Liow JS, Lu JQ, et al. Linearized reference tissue parametric imaging methods: application to [11C]DASB positron emission tomography studies of the serotonin transporter in human brain. J Cereb Blood Flow Metab 2003;23:1096-1112.
34. Kish SJ, Furukawa Y, Chang LJ, et al. Regional distribution of serotonin transporter protein in postmortem human brain - Is the cerebellum a SERT-free brain region? Nucl Med Biol 2005;32:123-128.
35. Ginovart N, Wilson AA, Meyer JH, Hussey D, Houle S. Positron emission tomography quantification of [(11)C]-DASB binding to the human serotonin transporter: modeling strategies. J Cereb Blood Flow Metab 2001;21: 1342-1353.
36. Morrish PK, Rakshi JS, Bailey DL, Sawle GV, Brooks DJ. Measuring the rate of progression and estimating the preclinical period of Parkinson's disease with [18F]dopa PET. J Neurol Neurosurg Psychiatry 1998;64:314-319.
37. Pirker W, Djamshidian S, Asenbaum S, et al. Progression of dopaminergic degeneration in Parkinson's disease and atypical parkinsonism: A longitudinal β-CIT SPECT study. Mov Disord 2002;17: 45-53.
38. Marek K, Innis R, van Dyck C, et al. [I-123]beta-CIT SPECT imaging assessment of the rate of Parkinson's disease progression. Neurology 2001;57:2089-2094.
39. Bruck A, Aalto S, Rauhala E, Bergman J, Marttila R, Rinne JO. A follow-up study on 6-[(18)F]fluoro-L-dopa uptake in early Parkinson's disease shows nonlinear progression in the putamen. Mov Disord 2009;24:1009-1015.
40. Nurmi E, Ruottinen HM, Bergman J, et al. Rate of progression in Parkinson's disease: A 6-[18F]fluoro-L-dopa PET study. Mov Disord 2001;16:608-615.
41. Ito K, Morrish PK, Bailey DL, et al. A comparison of the progression of early Parkinson's disease in patients started on ropinirole or L-dopa: an 18F-dopa PET study. J Neural Transm 2002;109: 1433-1443.

42. Whone AL, Watts RL, Stoessl AJ, et al. Slower progression of Parkinson's disease with ropinirole versus levodopa: the REAL-PET study. Ann Neurol 2003;54:93-101.
43. Parkinson Study Group. Pramipexole vs levodopa as initial treatment for Parkinson disease - A randomized controlled trial. JAMA 2000;284:1931-1938.
44. Fahn S, Parkinson Study Group. Does levodopa slow or hasten the rate of progression of Parkinson's disease? J Neurol 2005;252:37-42.
45. Politis M, Oertel WH, Wu K, et al. Graft-induced dyskinesias in Parkinson's disease: High striatal serotonin/dopamine transporter ratio. Mov Disord 2011;26:1997-2003.
46. Politis M, Wu K, Loane C, et al. Staging of serotonergic dysfunction in Parkinson's Disease: An in vivo 11C-DASB PET study. Neurobiol Dis 2010;40:216-221.
47. Delaville C, De Deurwaerdère P, Benazzouz A. Noradrenaline and Parkinson's disease. Front Syst Neurosci 2011;5:31.
48. Emond P, Garreau L, Chalon S, et al. Synthesis and ligand binding of nortropane derivatives: N-substituted 2beta-carbomethoxy-3beta-(4′-iodophenyl)nortropane and N-(3-iodoprop-(2E)-enyl)-2beta-carbomethoxy-3beta-(3′,4′-disubstituted phenyl)nortropane. New high-affinity and selective compounds for the dopamine transporter. J Med Chem 1997;40:1366-1372.
49. Chalon S, Emond P, Besnard J, et al. Visualization of the dopamine transporter in the human brain postmortem with the new selective ligand [125I]PE2I. Neuroimage 1999;9:108-116.
50. Halldin C, Erixon-Lindroth N, Pauli S, et al. [(11)C]PE2I: a highly selective radioligand for PET examination of the dopamine transporter in monkey and human brain. Eur J Nucl Med Mol Imaging 2003;30:1220-1230.
51. Zebell M, Holm-Hansen S, Thomsen G, et al. Serotonin transporters in dopamine transporter imaging: a head-to-head comparison of dopamine transporter SPECT radioligands 123I-FP-CIT and 123I-PE2I. J Nucl Med 2010;51:1885-1891.
52. Jucaite A, Odano I, Olsson H, Pauli S, Halldin C, Farde L. Quantitative analyses of regional [11C]PE2I binding to the dopamine transporter in the human brain: a PET study. Eur J Nucl Med Mol Imaging 2006;33:657-668.
53. Seki C, Ito H, Ichimiya T, et al. Quantitative analysis of dopamine transporters in human brain using [11C]PE2I and positron emission tomography: evaluation of reference tissue models. Ann Nucl Med 2010;24:249-260.
54. Appel L, Jonasson M, Danfors T, et al. Use of 11C-PE2I PET in differential diagnosis of parkinsonian disorders. J Nucl Med 2015;56:234-242.
55. Hughes AJ, Daniel SE, Kilford L, Lees AJ. Accuracy of clinical diagnosis of idiopathic Parkinson's disease: a clinico-pathological study of 100 cases. J Neurol Neurosurg Psychiatry 1992;55:181-184.
56. Goetz CG, Tilley BC, Shaftman SR, et al. Movement Disorder Society-sponsored revision of the Unified Parkinson's Disease Rating Scale (MDS-UPDRS): scale presentation and clinimetric testing results. Mov Disord 2008;23:2129-2170.
57. Garcia de Yebenes J, Fahn S. New therapeutic alternatives in Parkinson disease. Neurologia 1987;2:199-201.
58. Hoehn MM, Yahr MD. Parkinsonism: onset, progression and mortality. Neurology 1967;17:427-442.
59. Gunn R, Coello C, Searle G. Molecular Imaging And Kinetic Analysis Toolbox (MIAKAT) — a quantitative software package for the analysis of PET neuroimaging Data. J Nucl Med 2016;57:1928.
60. Jenkinson M, Beckmann CF, Behrens TE, Woolrich MW, Smith SM. FSL. Neuroimage 2012;62:782-790.
61. Mazziotta JC, Toga AW, Evans A, Fox P, Lancaster J. A probabilistic atlas of the human brain: theory and rationale for its development. The International Consortium for Brain Mapping (ICBM). Neuroimage 1995;2:89-101.
62. Tziortzi AC, Searle GE, Tzimopoulou S, et al. Imaging dopamine receptors in humans with [11C]-(+)-PHNO: dissection of D3 signal and anatomy. Neuroimage 2011;54:264-277.
63. Lammertsma AA, Hume SP. Simplified reference tissue model for PET receptor studies. Neuroimage 1996;4:153-158.
64. Patlak CS, Blasberg RG. Graphical evaluation of blood-to-brain transfer constants from multiple-time uptake data. Generalizations. J Cereb Blood Flow Metab 1985;5:584-590.
65. Kumakura Y, Vernaleken I, Grunder G, Bartenstein P, Gjedde A, Cumming P. PET studies of net blood-brain clearance of FDOPA to human brain: age-dependent decline of [18F]fluorodopamine storage capacity. J Cereb Blood Flow Metab 2005;25:807-819.
66. Steiger JH. Tests for comparing elements of a correlation matrix. Psychol Bull 1980;87:245-251.
67. Smith SM, Nichols TE. Threshold-free cluster enhancement: addressing problems of smoothing, threshold dependence and localisation in cluster inference. Neuroimage 2009;44:83-98.
68. Rinne JO, Ruottinen H, Bergman J, Haaparanta M, Sonninen P, Solin O. Usefulness of a dopamine transporter PET ligand [(18)F]beta-CFT in assessing disability in Parkinson's disease. J Neurol Neurosurg Psychiatry 1999;67:737-741.
69. Prunier C, Payoux P, Guilloteau D, et al. Quantification of dopamine transporter by 123I-PE2I SPECT and the noninvasive Logan graphical method in Parkinson's disease. J Nucl Med 2003;44:663-670.
70. Gunther I, Hall H, Halldin C, Swahn CG, Farde L, Sedvall G. [I-125]beta-CIT-FE and [I-125]beta-CIT-FP are superior to [I-125]beta-CIT for dopamine transporter visualization: Autoradiographic evaluation in the human brain. Nucl Med Biol 1997;24:629-634.
71. Booij J, de Jong J, de Bruin K, Knol R, de Win MM, van Eck-Smit BL. Quantification of striatal dopamine transporters with I-123-FP-CIT SPECT is influenced by the selective serotonin Reuptake inhibitor paroxetine: A double-blind, placebo-controlled, crossover study in healthy control subjects. J Nucl Med 2007;48:359-366.
72. Loane C, Politis M. Positron emission tomography neuroimaging in Parkinson's disease. Am J Transl Res 2011;3:323-341.
73. Guilloteau D, Emond P, Baulieu JL, et al. Exploration of the dopamine transporter: In vitro and in vivo characterization of a high-affinity and high-specificity iodinated tropane derivative (E)-N-(3-iodoprop-2-enyl)-2 beta-carbomethoxy-3 beta-(4 ′-methylphenyl)-nortropane (PE2I). Nucl Med Biol 1998;25:331-337.
74. McDermott M, Shinaman A, Kamp C, et al. Pramipexole vs levodopa as initial treatment for Parkinson disease - A 4-year randomized controlled trial. Arch Neurol 2004;61:1044-1053.
75. Oikonen V, Lumme V, Virsu P, et al. Measurement of striatal and extrastriatal dopamine transporter binding with high-resolution PET and [11C]PE2I: quantitative modeling and test-retest reproducibility. J Cereb Blood Flow Metab 2008;28:1059-1069.
76. Egerton A, Demjaha A, McGuire P, Mehta MA, Howes OD. The test-retest reliability of 18F-DOPA PET in assessing striatal and extrastriatal presynaptic dopaminergic function. Neuroimage 2010;50:5245-31.

Supporting Data

Additional Supporting Information may be found in the online version of this article at the publisher's website.